 doi:10.20944/preprints202410.0572.v1

Article

An Anti-Human EphA2 Monoclonal Antibody Ea2Mab-7 Shows High Sensitivity for Flow Cytometry, Western Blot, and Immunohistochemical Analyses

Hiroyuki Satofuka, Hiroyuki Suzuki, Tomohiro Tanaka, Guanjie Li, Mika K. Kaneko and Yukinari Kato *

Department of Antibody Drug Development, Tohoku University Graduate School of Medicine, 2-1 Seiryo-machi, Aoba-ku, Sendai, Miyagi 980-8575, Japan

* Correspondence: yukinari.kato.e6@tohoku.ac.jp (Y.K.); Tel.: +81-22-717-8207

Abstract: Ephrin type A receptor 2 (EphA2) binds to membrane-bound ligands, ephrin A1, A2, and A5, eliciting bidirectional signaling. This signaling regulates many physiological processes, such as tissue development, homeostasis, and regeneration. The dysregulation of the EphA2-ephrins axis contributes to various diseases, including cancers. The high expression of EphA2 is observed in various cancers, which promotes cancer malignancy, whereas its levels are relatively low in most normal adult tissues. Therefore, EphA2 is a promising target for cancer therapy. In this study, we developed anti-human EphA2 monoclonal antibodies using the Cell-Based Immunization and Screening method. Among them, a clone Ea2Mab-7 (IgG_1, κ) exhibited a high affinity and sensitivity in flow cytometry. The dissociation constant values of Ea2Mab-7 for CHO/EphA2 and MDA-MB-231 cells were determined as 7.7×10^{-9} M and 2.1×10^{-9} M, respectively. Furthermore, Ea2Mab-7 can detect endogenous EphA2 in western blot and immunohistochemistry. Therefore, the Ea2Mab-7 is highly versatile for basic research and is expected to contribute to clinical applications, such as antibody therapy and tumor diagnosis.

Keywords: EphA2; monoclonal antibody; cell-based immunization and screening; flow cytometry; immunohistochemistry; breast cancer

1. Introduction

Ephrin receptors (Eph) have a single transmembrane domain and are grouped into A and B categories based on their extracellular domains, which determine the binding affinity for ligands [1,2]. The interaction of Eph with the membrane-bound ephrin-A family ligands mediates communication between cells of the same or different types, and contact-dependent bidirectional (forward and reverse) signaling spreads from adjacent cells to neighboring cells [3–5]. The bidirectional signaling of the Eph system plays critical roles in tissue development, homeostasis, and regeneration.

EphA2 has been studied extensively in tumor development and progression [6]. Abundant expression of EphA2 has been reported in various cancers such as prostate [7], lung [8], esophageal [9], colorectal [10], cervical [11], ovarian [12], skin [13], and breast cancers [14]. It is correlated with the malignancy [15]. EphA2 expression is associated with poor prognosis, elevated metastatic potential, and reduced patient survival [16,17]. Notably, the expression of EphA2 protein and mRNA was correlated with lymph node metastasis, clinical stage, and histologic grade of breast cancer [18]. Therefore, EphA2 is a promising target in cancer therapy because of its relatively low levels in most normal adult tissues [3].

Monoclonal antibody (mAb) therapy targeting EphA2 has been developed based on evidence that ligand stimulation, such as ephrin A1, is sufficient to induce EphA2 degradation through internalization [19]. For instance, anti-EphA2 mAbs (EA2 and B233) promoted EphA2

 doi:10.20944/preprints202410.0572.v1

phosphorylation and degradation in cancer cells, and administration of EA2 mAb significantly decreased tumor growth in xenograft model [20]. In addition, a single-chain Fv of anti-EphA2 mAb (D2) blocked the ligand interaction in COS-7 cells and induced apoptosis in the lymphoma cell line [21]. An anti-EphA2 mAb (SHM16) does not inhibit the interaction between ephrin A1 and EphA2 [22]. However, SHM16 stimulates the internalization of EphA2 and inhibits malignant features of melanoma A375 cells. A humanized anti-EphA2 mAb (DS-8895a) was developed as a therapeutic mAb with antibody-dependent cellular cytotoxicity (ADCC). Treatment with DS-8895a inhibited tumor growth of EphA2-positive human breast and gastric cancers in xenograft model [23]. Anti-EphA2 mAb-based immunotherapy using chimeric antigen receptor-T cells has also been developed and is undergoing clinical trials [24,25].

We have developed various mAbs against membrane proteins using the Cell-Based Immunization and Screening (CBIS) method [26–33]. The mAbs obtained by this method are prone to recognize conformational epitopes and are suitable for flow cytometry. Furthermore, some of these mAbs are also available for western blot, immunocytochemistry (ICC), and immunohistochemistry (IHC). This allows simultaneous contributions to the development of both therapy and diagnosis. Among the anti-EphA2 mAbs developed to date, SHM16 is known to recognize intact structures on the cell surface, while mAbs such as D4A2 are suitable only for western blot and IHC [34,35]. Anti-EphA2 mAbs available for flow cytometry, western blot, ICC, and IHC have not been reported (Supplementary Table S1). This study employed the CBIS method to generate a highly versatile anti-EphA2 mAb.

2. Materials and Methods

2.1. Cell Lines

Chinese hamster ovary (CHO)-K1, P3X63Ag8.U1 (P3U1), human glioblastoma LN229, and human breast cancer MDA-MB-231 were obtained from American Type Culture Collection (ATCC, Manassas, VA, USA). The human pancreas cancer MIA PaCa-2 and colorectal cancer HCT-15 were obtained from the Cell Resource Center at Tohoku University (Miyagi, Japan). The human lung cancer PC-10 was obtained from Immuno-Biological Laboratories Co., Ltd. (Gunma, Japan).

MDA-MB-231, MIA PaCa-2, HCT-15, LN229, and LN229/EphA2 were maintained in DMEM. CHO-K1, CHO/EphA2, P3U1, and PC-10 were maintained in RPMI-1640 medium (Nacalai Tesque, Inc., Kyoto, Japan). The media were supplied with 10% heat-inactivated fetal bovine serum (FBS; Thermo Fisher Scientific, Inc., Waltham, MA, USA) and 100 U/mL penicillin, 100 μg/mL streptomycin, 0.25 μg/mL amphotericin B (Nacalai Tesque).

2.2. Plasmid Construction and Establishment of Stable Transfectants

The genes encoding human *EPHA2* (NM_004431) was subcloned into the pCAG-Ble vector (FUJIFILM Wako Pure Chemical Corporation, Osaka, Japan). The EphA2 overexpressed CHO-K1 and LN229 were generated using anti-EphA2 mAb, SHM16 (mouse IgG_{2b}, κ, BioLegend, San Diego, CA, USA) and a SH800 cell sorter (Sony Corporation, Tokyo, Japan).

2.3. Development of Hybridomas

The female BALB/cAJcl mice were purchased from CLEA Japan (Tokyo, Japan). The mice were intraperitoneally immunized with LN229/EphA2 cells (1×10^8 cells/injection) and Alhydrogel adjuvant 2% (InvivoGen). After four additional immunizations with LN229/EphA2 cells, the hybridomas were generated by fusing the spleen cells with P3U1 cells using polyethylene glycol 1500 (Roche Diagnostics, Indianapolis, IN, USA).

 doi:10.20944/preprints202410.0572.v1

2.4. Flow Cytometric Analysis

Cells were detached and harvested using 1 mM ethylenediaminetetraacetic acid (EDTA; Nacalai Tesque, Inc.) to prevent enzymatic degradation of cell surface proteins. The cells were washed with 0.1% bovine serum albumin (BSA) in phosphate-buffered saline (PBS, blocking buffer) and stained with mAbs by incubating for 30 minutes at 4°C. Subsequently, the cells were stained with Alexa Fluor 488-conjugated anti-mouse IgG (2,000-fold dilution; Cell Signaling Technology, Inc., Danvers, MA, USA) for 30 minutes at 4°C. The data were collected using the SA3800 Cell Analyzer and analyzed using FlowJo software (BD Biosciences, Franklin Lakes, NJ, USA).

2.5. Determination of Dissociation Constant (K_D) by Flow Cytometry

CHO/EphA2 and MDA-MB-231 cells were treated with serially diluted Ea$_2$Mab-7 and SHM16 (0.005–10 μg/mL). Subsequently, the cells were stained with Alexa Fluor 488-conjugated anti-mouse IgG (200-fold dilution) for 30 minutes at 4°C. The data were collected using the SA3800 Cell Analyzer and analyzed using FlowJo software. The fitting binding isotherms determined the dissociation constant (K_D) values to built-in one-side binding models of GraphPad Prism 6 (GraphPad Software, Inc. La Jolla, CA, USA).

2.6. Western Blot Analysis

Whole cell lysate (10 μg of protein per lane) was separated into 5–20% polyacrylamide gels (FJIFILM Wako Pure Chemical Corporation) and transferred onto polyvinylidene difluoride (PVDF) membranes (Merck KGaA, Darmstadt, Germany). After blocking with 4% skim milk (Nacalai Tesque, Inc.) in PBST, the membranes were incubated with 1 μg/mL of Ea$_2$Mab-7, SHM16, or an anti-β-actin mAb (clone AC-15; Sigma-Aldrich Corporation, St. Louis, MO, USA). Subsequently, they were incubated with anti-mouse IgG conjugated with horseradish peroxidase (1,000-fold dilution; Agilent Technologies, Inc., Santa Clara, CA, USA). Chemiluminescence signals were developed with ImmunoStar LD (FUJIFILM Wako Pure Chemical Corporation) or Pierce ECL Plus Western Blotting Substrate (Thermo Fisher Scientific, Inc.) and detected using a Sayaca-Imager (DRC Co., Ltd., Tokyo, Japan).

2.7. Immunocytochemical Analysis (ICC)

Cell blocks were prepared using iPGell (Genostaff Co., Ltd., Tokyo, Japan). The paraffin-embedded cell sections were autoclaved in a citrate buffer (pH 6.0; Nichirei Biosciences, Inc., Tokyo, Japan). After blocking using the SuperBlock T20 Blocking Buffer (Thermo Fisher Scientific Inc.), the sections were incubated with 10 μg/mL of Ea$_2$Mab-7, and then treated with the Envision+ Kit (Agilent Technologies Inc.). Color was developed using 3,3′-diaminobenzidine tetrahydrochloride (Agilent Technologies Inc.), and counterstaining was performed using hematoxylin (Merck KGaA, Darmstadt, Germany).

2.8. Immunohistochemical Analysis (IHC)

Formalin-fixed paraffin-embedded (FFPE) breast invasive ductal carcinoma tissue array (Cat. No.: BR729) containing 71 cases was purchased (FUJIFILM Wako Pure Chemical Corporation). The section was stained with Ea$_2$Mab-7 (10 μg/mL) using *BenchMark* ULTRA *PLUS (Roche Diagnostics*, Indianapolis, IN*).*

3. Results

3.1. Development of Anti-Human EphA2 mAbs

Two BALB/cAJcl mice were immunized with LN229/EphA2 cells, and the generated hybridomas were seeded into 96-well plates. After forming colonies, supernatants were collected and analyzed by flow cytometry-based high throughput screening to determine supernatants that were negative

 doi:10.20944/preprints202410.0572.v1

for CHO-K1 and positive for CHO/EphA2. Subsequently, anti-EphA2 mAb-producing hybridomas were cloned by limiting dilution. Finally, a clone Ea2Mab-7 (IgG1, κ) was established (Figure 1).

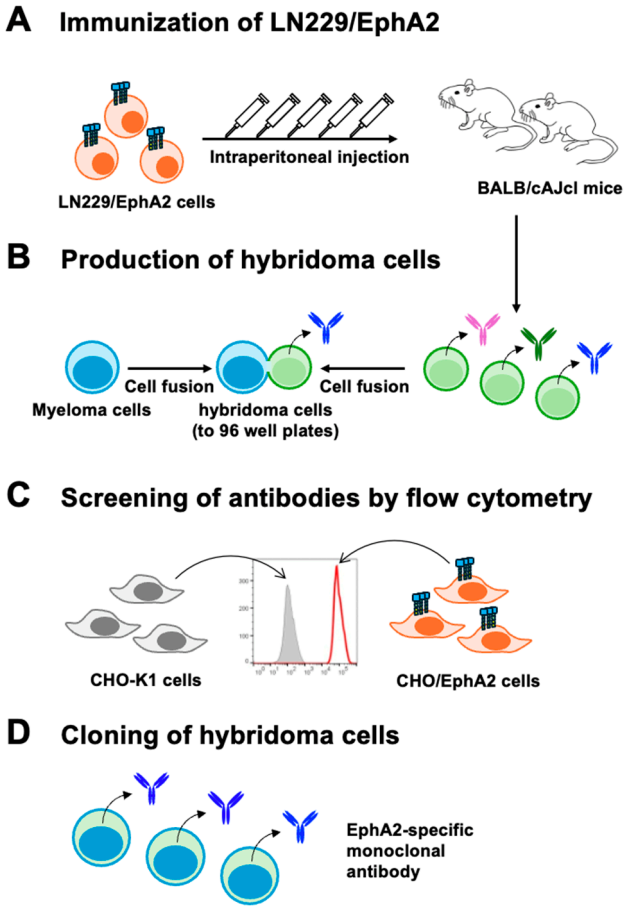

Figure 1. Schematic illustration of anti-EphA2 mAbs production. (A) LN229/EphA2 cells were intraperitoneally injected into BALB/cAJcl mice. (B) After immunization, spleen cells were collected and fused with P3U1. (C) The supernatants of hybridoma cells were screened to obtain anti-EphA2 specific mAbs by flow cytometry using CHO/EphA2 and parental CHO-K1 cells. (D) Antigen-specific mAb-producing hybridoma cells were established by the limiting dilution method.

3.2. Flow Cytometry

We conducted flow cytometry using Ea2Mab-7 against CHO/EphA2 and CHO-K1 cells. Ea2Mab-7 recognized CHO/EphA2 cells in a dose-dependent manner, ranging from 10 to 0.005 μg/mL, but did not bind to CHO-K1 cells at any concentrations (Figure 2A), indicating Ea2Mab-7 specifically recognizes EphA2 on the cell surface. A commercially available anti-EphA2 mAb (SHM16) exhibited a similar reactivity against CHO/EphA2 and CHO-K1 cells compared to Ea2Mab-7 (Figure 2B). We next investigated the reactivity of Ea2Mab-7 against endogenously EphA2-expressing cell lines, MDA-MB-231, MIA PaCa-2, HCT-15, PC-10, and LN229. Ea2Mab-7 and SHM16 reacted with these cell lines at 10 μg/mL (Figure 3).

 doi:10.20944/preprints202410.0572.v1

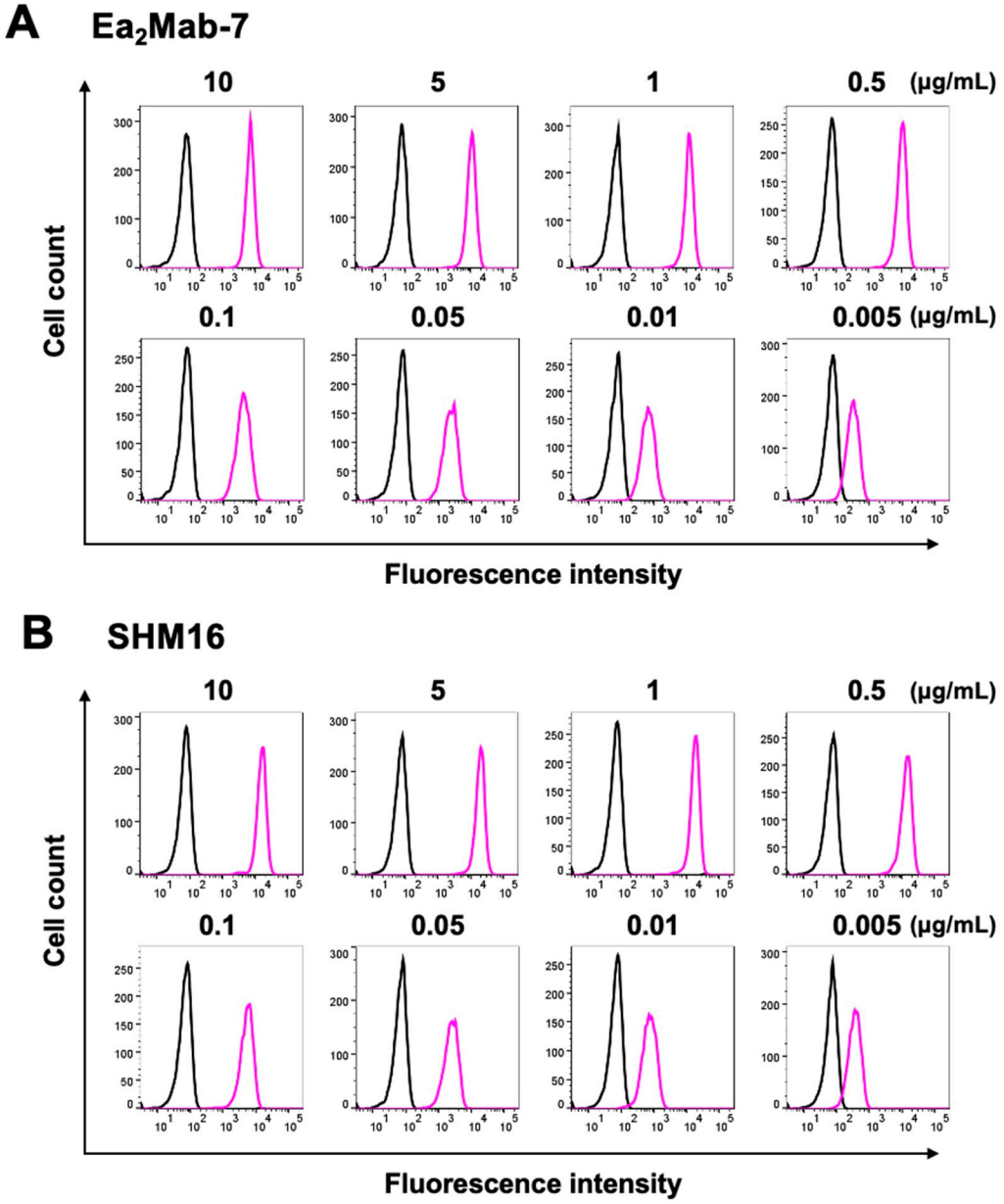

Figure 2. Flow cytometry of anti-EphA2 mAbs against CHO/EphA2 and CHO-K1 cells. CHO-K1 (black lines) and CHO/EphA2 (Purple lines) cells were treated with Ea_2Mab-7 (A) and a commercially available anti-EphA2 mAb, SHM16 (B) at the indicated concentrations. The mAbs-treated cells were incubated with anti-mouse IgG conjugated with Alexa Fluor 488. The fluorescence data were subsequently collected using the SA3800 Cell Analyzer.

 doi:10.20944/preprints202410.0572.v1

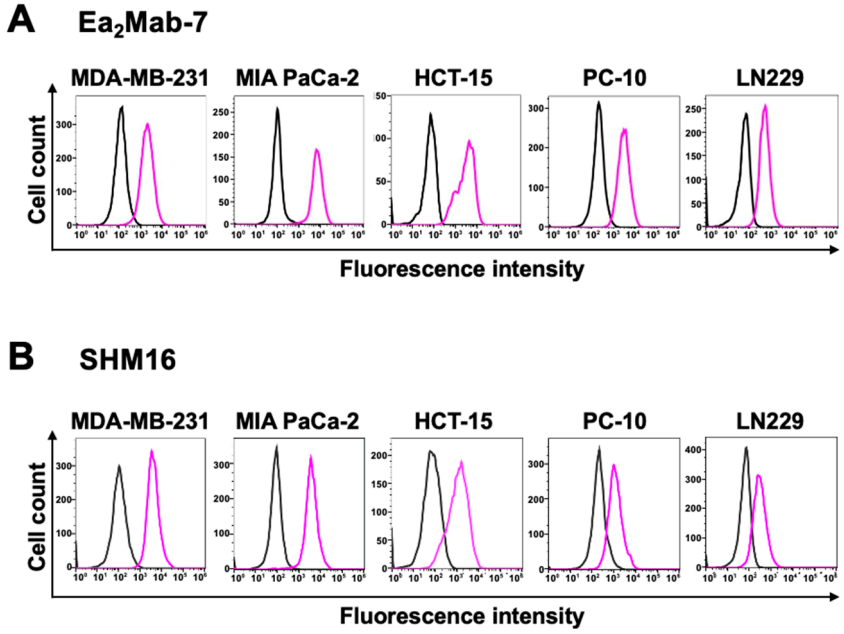

Figure 3. Flow cytometry of anti-EphA2 mAbs against endogenous EphA2 expressing cancer cells. MDA-MB-231, MIA PaCa-2, HCT-15, PC-10, and LN229 cells were treated with Ea2Mab-7 (A, Purple lines) and a commercially available anti-EphA2 mAb, SHM16 (B, Purple lines) at the indicated concentrations. The mAbs-treated cells were incubated with anti-mouse IgG conjugated with Alexa Fluor 488. The fluorescence data were subsequently collected using the SA3800 Cell Analyzer. The black line represents the negative control (blocking buffer).

3.3. Determination of KD Values

We performed flow cytometry to determine the binding affinity and calculated the *K*D values of Ea2Mab-7 and SHM16. The *K*D values of Ea2Mab-7 for CHO/EphA2 and MDA-MB-231 cells were 7.7 × 10^{-9} M and 2.1 × 10^{-9} M, respectively (Figure 4). The *K*D values of SHM16 for CHO/EphA2 and MDA-MB-231 were 8.4 × 10^{-9} M and 2.3 × 10^{-9} M, respectively. These results indicated that the affinity of Ea2Mab-7 is slightly higher than that of SHM16.

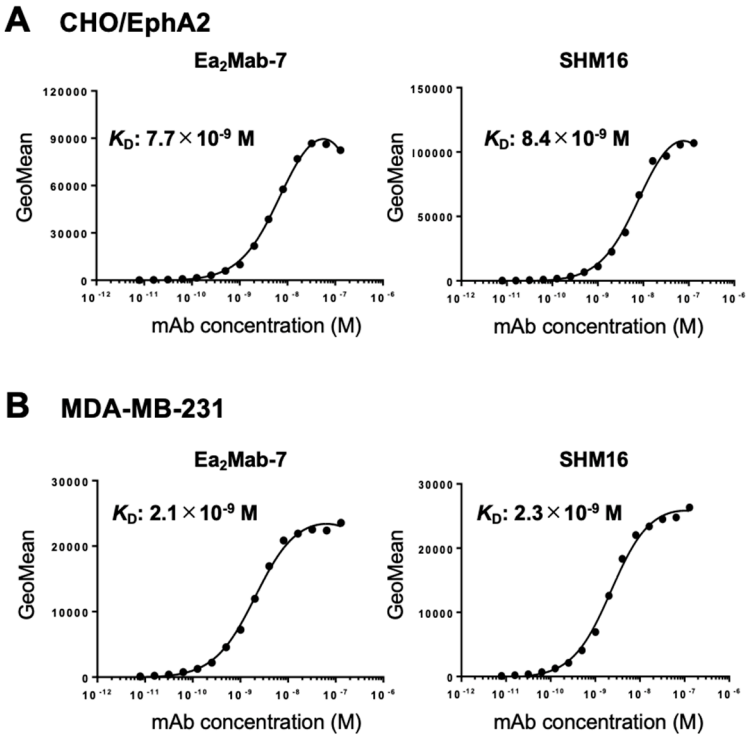

 doi:10.20944/preprints202410.0572.v1

Figure 4. Measurement of binding affinity of Ea2Mab-7 and SHM16. CHO/EphA2 cells (A) and MDA-MB-231 cells (B) were stained with mAbs serially diluted at the indicated concentrations. The fluorescence data were subsequently collected using the SA3800 Cell Analyzer, followed by the calculation of the K_D using GraphPad PRISM 6.

3.4. Western Blot Analysis

We next investigated whether Ea2Mab-7 is available for western blot. Whole cell lysate of CHO-K1, CHO/EphA2, MDA-MB-231, MIA PaCa-2, HCT-15, PC-10, and LN229 were also analyzed. Ea2Mab-7 showed a clear signal around the estimated molecular weight (108 kDa) of EphA2 in CHO/EphA2 (Supplementary Figure S1A and Figure 5A). In contrast, SHM16 was not available for western blot (Supplementary Figure S1B). Furthermore, Ea2Mab-7 is also capable of detecting endogenous EphA2 of MDA-MB-231, MIA PaCa-2, and HCT-15 (Figure 5A). Weak signal was detected in PC-10 and LN229 (Figure 5A).

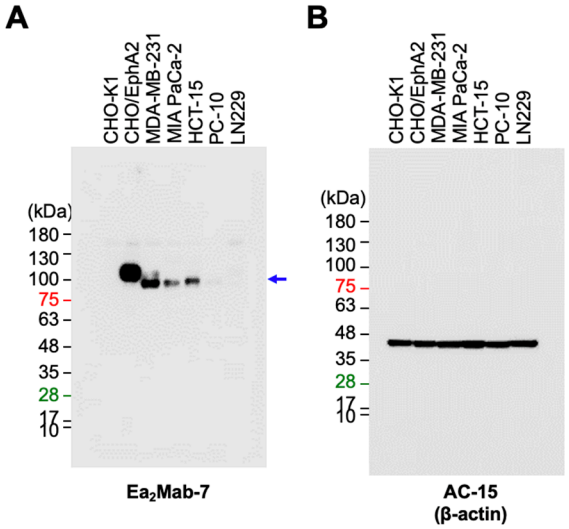

Figure 5. Western blot analysis using Ea2Mab-7. The cell lysate (10 μg/lane) of CHO-K1, CHO/EphA2, MDA-MB-231, MIA PaCa-2, HCT-15, PC-10, and LN229 cells were electrophoresed and transferred onto PVDF membranes. The membranes were incubated with 1 μg/mL of Ea2Mab-7 (A) and 0.5 μg/mL of AC-15 (anti-β-actin mAb) (B). The blue arrow indicates the estimated molecular weights of EphA2 (108.3 kDa).

3.5. ICC

To investigate whether Ea2Mab-7 can be used for ICC analyses, paraffin-embedded CHO-K1 and CHO/EphA2 sections were stained with Ea2Mab-7. Apparent membranous staining by Ea2Mab-7 was observed in CHO/EphA2 (Figure 6A) but not in CHO-K1 (Figure 6B). These results indicate the usefulness of Ea2Mab-7 for detecting EphA2-positive cells in paraffin-embedded cell samples.

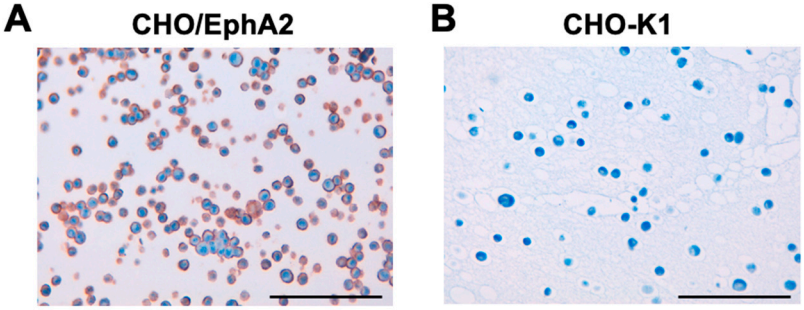

Figure 6. ICC of the paraffin-embedded cell sections of CHO-K1 and CHO/EphA2. The sections of CHO/EphA2 (A) and CHO-K1 (B) cells were treated with 10 μg/mL of Ea2Mab-7, followed by that

 doi:10.20944/preprints202410.0572.v1

with the Envision + Kit. Color was developed using DAB, and counterstaining was performed using hematoxylin (Merck KGaA, Darmstadt, Germany). Scale bar = 100 μm.

3.6. IHC

Next, the FFPE breast cancer tissue array was stained with Ea2Mab-7. The cytoplasmic pattern of EphA2 staining was observed. We classified the results into strong positive (2+, Figure 7A), positive (1+, Figure 7B), and negative (0, Figure 7B). The staining results were summarized in Supplementary Table S2.

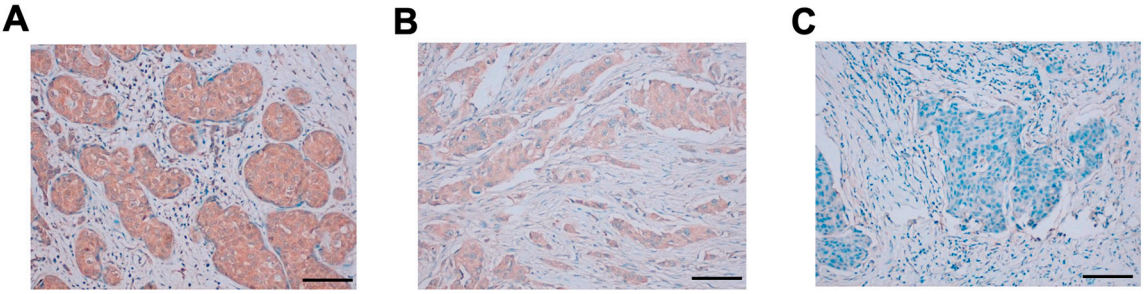

Figure 7. IHC using Ea_2Mab-7 against breast cancer tissues. The sections of breast cancer tissue array (BR729) were treated with 10 μg/mL of Ea_2Mab-7. The staining was carried out using VENTANA BenchMark Ultra (Roche Diagnostics Corporation, IN, USA). Scale bar = 100 μm.

4. Discussion

In this study, we established a novel anti-EphA2 mAb, Ea_2Mab-7, which is the first mAb available to various applications, including flow cytometry (Figs. 2–4), western blot (Figure 5), ICC (Figure 6), and IHC (Figure 7). We established twelve clones during the establishment of anti-EphA2 mAbs by the CBIS method. However, Ea_2Mab-7 is the sole mAb available to all applications. Although SHM16 was established by the immunization of A375 melanoma cells into mice [22], SHM16 was not available to western blot (Supplementary Figure 1). Therefore, the identification of the epitope of Ea_2Mab-7 is essential to reveal the structural basis of antigen recognition by Ea_2Mab-7. We have developed the PA insertion for epitope mapping (PAMAP) and RIEDL insertion for epitope mapping (REMAP) to determine the epitope of mAbs [36–40]. The epitopes of anti-mouse CD39 mAb (C_{39}Mab-1) could be determined using both REMAP and PAMAP methods [36]. Furthermore, the epitopes of anti-CD44 mAbs (C_{44}Mab-5 and C_{44}Mab-46) [37,38] and anti-EGFR mAbs (EMab-51 and EMab-134) [39,40] could be determined using the REMAP method. Therefore, further studies are required to determine the epitope of Ea_2Mab-7. If Ea_2Mab-7 possesses the linear and non-glycosylated epitope, it may contribute to developing highly versatile mAbs to other Eph families using peptide immunization of the corresponding sequence.

Interaction between EphA2 and ephrin-As anchored on the plasma membranes of adjacent cells induces the large oligomeric complexes that mediate bidirectional signaling [5]. In contrast, the ephrin-A-independent non-canonical signaling of EphA2 plays a critical role in cancer progression [3]. The serine-threonine kinases of the RSK family [41] and AKT [42] can induce the phosphorylation of EphA2 (S897), which mediates oncogenic transformation [43], metabolic reprogramming [44], invasion [45], and resistance to therapies [8,46]. Furthermore, phosphorylated EphA2 (S897) has been shown to correlate with poor prognosis of breast cancer patients [47]. Therefore, anti-EphA2 mAbs can target cancer cells, which activate the non-canonical EphA2 signaling. To target the EphA2-positive cancer cells by Ea_2Mab-7 (IgG_1), we should generate a class-switched mouse IgG_{2a} mAb from mouse IgG_1. Furthermore, we previously produced defucosylated IgG_{2a} type mAbs to enhance the ADCC and *in vivo* antitumor effect in mouse xenograft models [48,49]. The class-switched and defucosylated type Ea_2Mab-7 could contribute to treating EphA2-positive cancers in preclinical studies.

Focusing on the detailed signal intensities, different correlations are observed between applications. For instance, the western blot signal did not wholly match the flow cytometry signal

 doi:10.20944/preprints202410.0572.v1

intensity (Figures 3A and 5A). Clear signals for CHO/EphA2, MDA-MB-231, MIA PaCa-2, and HCT-15 cells were detected in both flow cytometry and western blot. However, weak or nearly undetectable signals were observed in PC-10 and LN229 cells in the western blot, while clear signals were detected in flow cytometry. Western blot shows the total amount of EphA2 expression in whole cells. At the same time, flow cytometry indicates the amount of EphA2 on the cell surface, suggesting that intracellular and extracellular levels of EphA2 differ depending on the cell line. This discrepancy may help explain the malignancy of cancer cells, as the abundant expression of EphA2 on the cell surface enables the triggering of non-canonical signaling that promotes cancer cell growth [3,19,50]. Additionally, compared to CHO/EphA2 cells, the signals of the endogenously expressed cell lines show a slightly smaller molecular weight in western blot, which may be due to the alternative splicing of EphA2 [51]. Therefore, mAbs, available for various applications, such as western blot and flow cytometry, provide significant advantages in estimating intracellular and extracellular protein levels and detecting protein processing.

Ea$_2$Mab-7 can detect exogenous and endogenous EphA2 in ICC and IHC analysis (Figs. 6 and 7). We could detect apparent membranous staining in the CHO/EphA2 section (Figs. 6). In contrast, IHC analysis of the breast cancer tissue array mainly showed cytoplasmic staining in most cases (Figs. 7 and Supplementary Table S2). This result was consistent with the previous reports using several anti-EphA2 Abs [35,52,53]. EphA2 was shown to receive the ligand-induced internalization [54]. Furthermore, the activation of receptor tyrosine kinase MET can induce the phosphorylation of EphA2 (S897) and endosomal internalization [55]. It would be interesting to investigate whether the cytoplasmic localization of EphA2 is involved in the malignant properties of cancer cells.

In conclusion, Ea$_2$Mab-7 is a highly sensitive and versatile mAb for basic research and is expected to contribute to clinical applications such as antibody therapy and tumor diagnosis.

Supplementary Materials: The following supporting information can be downloaded at the website of this paper posted on Preprints.org.

Author Contributions: **Hiroyuki Satofuka**: Investigation, Writing – original draft; **Hiroyuki Suzuki**: Investigation, Funding acquisition; **Tomohiro Tanaka:** Investigation, Funding acquisition; **Guanjie Li:** Investigation; **Mika K. Kaneko:** Conceptualization, Funding acquisition; **Yukinari Kato:** Conceptualization, Funding acquisition, Project administration, Writing – review and editing; All authors have read and agreed to the published version of the manuscript

Funding: This research was supported in part by Japan Agency for Medical Research and Development (AMED) under Grant Numbers: JP24am0521010 (to Y.K.), JP24ama121008 (to Y.K.), JP23am0401013 (to Y.K.), JP24ama221339 (to Y.K.), JP24bm1123027 (to Y.K.), and JP24ck0106730 (to Y.K.), and by the Japan Society for the Promotion of Science (JSPS) Grants-in-Aid for Scientific Research (KAKENHI) grant nos. 24K11652 (to H.Satofuka), 22K06995 (to H.Suzuki), 21K20789 (to T.T.), 21K07168 (to M.K.K.), and 22K07224 (to Y.K.).

Institutional Review Board Statement: The animal study protocol was approved by the Animal Care and Use Committee of Tohoku University (Permit number: 2022MdA-001) for studies involving animals.

Informed Consent Statement: Not applicable.

Data Availability Statement: All related data and methods are presented in this paper. Additional inquiries should be addressed to the corresponding authors.

Conflicts of Interest: The authors declare no conflict of interest involving this article.

References

1. Biao-xue, R.; Xi-guang, C.; Shuan-ying, Y.; Wei, L.; Zong-juan, M. EphA2-dependent molecular targeting therapy for malignant tumors. *Curr Cancer Drug Targets* 2011;*11*(9): 1082-1097.
2. Tandon, M.; Vemula, S.V.; Mittal, S.K. Emerging strategies for EphA2 receptor targeting for cancer therapeutics. *Expert Opin Ther Targets* 2011;*15*(1): 31-51.
3. Pasquale, E.B. Eph receptors and ephrins in cancer progression. *Nat Rev Cancer* 2024;*24*(1): 5-27.
4. Pasquale, E.B. Eph receptor signalling casts a wide net on cell behaviour. *Nat Rev Mol Cell Biol* 2005;*6*(6): 462-475.

 doi:10.20944/preprints202410.0572.v1

5. Pasquale, E.B. Eph receptors and ephrins in cancer: bidirectional signalling and beyond. *Nat Rev Cancer* 2010;*10*(3): 165-180.
6. Zhou, Y.; Sakurai, H. Emerging and Diverse Functions of the EphA2 Noncanonical Pathway in Cancer Progression. *Biol Pharm Bull* 2017;*40*(10): 1616-1624.
7. Kurose, H.; Ueda, K.; Kondo, R.; et al. Elevated Expression of EPHA2 Is Associated With Poor Prognosis After Radical Prostatectomy in Prostate Cancer. *Anticancer Res* 2019;*39*(11): 6249-6257.
8. Amato, K.R.; Wang, S.; Tan, L.; et al. EPHA2 Blockade Overcomes Acquired Resistance to EGFR Kinase Inhibitors in Lung Cancer. *Cancer Res* 2016;*76*(2): 305-318.
9. Miyazaki, T.; Kato, H.; Fukuchi, M.; Nakajima, M.; Kuwano, H. EphA2 overexpression correlates with poor prognosis in esophageal squamous cell carcinoma. *Int J Cancer* 2003;*103*(5): 657-663.
10. Martini, G.; Cardone, C.; Vitiello, P.P.; et al. EPHA2 Is a Predictive Biomarker of Resistance and a Potential Therapeutic Target for Improving Antiepidermal Growth Factor Receptor Therapy in Colorectal Cancer. *Mol Cancer Ther* 2019;*18*(4): 845-855.
11. Wu, D.; Suo, Z.; Kristensen, G.B.; et al. Prognostic value of EphA2 and EphrinA-1 in squamous cell cervical carcinoma. *Gynecol Oncol* 2004;*94*(2): 312-319.
12. Lin, Y.G.; Han, L.Y.; Kamat, A.A.; et al. EphA2 overexpression is associated with angiogenesis in ovarian cancer. *Cancer* 2007;*109*(2): 332-340.
13. Mo, J.; Zhao, X.; Dong, X.; et al. Effect of EphA2 knockdown on melanoma metastasis depends on intrinsic ephrinA1 level. *Cell Oncol (Dordr)* 2020;*43*(4): 655-667.
14. Youngblood, V.M.; Kim, L.C.; Edwards, D.N.; et al. The Ephrin-A1/EPHA2 Signaling Axis Regulates Glutamine Metabolism in HER2-Positive Breast Cancer. *Cancer Res* 2016;*76*(7): 1825-1836.
15. Wykosky, J.; Debinski, W. The EphA2 receptor and ephrinA1 ligand in solid tumors: function and therapeutic targeting. *Mol Cancer Res* 2008;*6*(12): 1795-1806.
16. Kinch, M.S.; Moore, M.B.; Harpole, D.H. Predictive value of the EphA2 receptor tyrosine kinase in lung cancer recurrence and survival. *Clin Cancer Res* 2003;*9*(2): 613-618.
17. Garcia-Monclús, S.; López-Alemany, R.; Almacellas-Rabaiget, O.; et al. EphA2 receptor is a key player in the metastatic onset of Ewing sarcoma. *Int J Cancer* 2018;*143*(5): 1188-1201.
18. Zhou, L.; Lu, X.; Zhang, B.; Shi, Y.; Li, Z. EphA2 as a new target for breast cancer and its potential clinical application. *Int J Clin Exp Pathol* 2021;*14*(4): 484-492.
19. Xiao, T.; Xiao, Y.; Wang, W.; et al. Targeting EphA2 in cancer. *J Hematol Oncol* 2020;*13*(1): 114.
20. Coffman, K.T.; Hu, M.; Carles-Kinch, K.; et al. Differential EphA2 epitope display on normal versus malignant cells. *Cancer Res* 2003;*63*(22): 7907-7912.
21. Goldgur, Y.; Susi, P.; Karelehto, E.; et al. Generation and characterization of a single-chain anti-EphA2 antibody. *Growth Factors* 2014;*32*(6): 214-222.
22. Sakamoto, A.; Kato, K.; Hasegawa, T.; Ikeda, S. An Agonistic Antibody to EPHA2 Exhibits Antitumor Effects on Human Melanoma Cells. *Anticancer Res* 2018;*38*(6): 3273-3282.
23. Burvenich, I.J.; Parakh, S.; Gan, H.K.; et al. Molecular Imaging and Quantitation of EphA2 Expression in Xenograft Models with 89Zr-DS-8895a. *J Nucl Med* 2016;*57*(6): 974-980.
24. Yi, Z.; Prinzing, B.L.; Cao, F.; Gottschalk, S.; Krenciute, G. Optimizing EphA2-CAR T Cells for the Adoptive Immunotherapy of Glioma. *Mol Ther Methods Clin Dev* 2018;*9*: 70-80.
25. Li, N.; Liu, S.; Sun, M.; et al. Chimeric Antigen Receptor-Modified T Cells Redirected to EphA2 for the Immunotherapy of Non-Small Cell Lung Cancer. *Transl Oncol* 2018;*11*(1): 11-17.
26. Asano, T.; Nanamiya, R.; Takei, J.; et al. Development of Anti-Mouse CC Chemokine Receptor 3 Monoclonal Antibodies for Flow Cytometry. *Monoclon Antib Immunodiagn Immunother* 2021;*40*(3): 107-112.
27. Nanamiya, R.; Takei, J.; Asano, T.; et al. Development of Anti-Human CC Chemokine Receptor 9 Monoclonal Antibodies for Flow Cytometry. *Monoclon Antib Immunodiagn Immunother* 2021;*40*(3): 101-106.
28. Nanamiya, R.; Suzuki, H.; Kaneko, M.K.; Kato, Y. Development of an Anti-EphB4 Monoclonal Antibody for Multiple Applications Against Breast Cancers. *Monoclon Antib Immunodiagn Immunother* 2023;*42*(5): 166-177.
29. Saito, M.; Suzuki, H.; Tanaka, T.; et al. Development of an Anti-Mouse CCR8 Monoclonal Antibody (C. *Monoclon Antib Immunodiagn Immunother* 2022;*41*(6): 333-338.
30. Suzuki, H.; Tanaka, T.; Li, G.; et al. Development of a Sensitive Anti-Mouse CCR5 Monoclonal Antibody for Flow Cytometry. *Monoclon Antib Immunodiagn Immunother* 2024;*43*(4): 96-100.

31. Tanaka, T.; Nanamiya, R.; Takei, J.; et al. Development of Anti-Mouse CC Chemokine Receptor 8 Monoclonal Antibodies for Flow Cytometry. *Monoclon Antib Immunodiagn Immunother* 2021;*40*(2): 65-70.
32. Tateyama, N.; Asano, T.; Suzuki, H.; et al. Epitope Mapping of Anti-Mouse CCR3 Monoclonal Antibodies Using Flow Cytometry. *Antibodies (Basel)* 2022;*11*(4).
33. Yoshida, S.; Kato, T.; Kanno, N.; et al. Cell type-specific localization of Ephs pairing with ephrin-B2 in the rat postnatal pituitary gland. *Cell Tissue Res* 2017;*370*(1): 99-112.
34. Yasuta, Y.; Kaminaka, R.; Nagai, S.; et al. Cooperative function of oncogenic MAPK signaling and the loss of Pten for melanoma migration through the formation of lamellipodia. *Sci Rep* 2024;*14*(1): 1525.
35. Nikas, I.; Giaginis, C.; Petrouska, K.; et al. EPHA2, EPHA4, and EPHA7 Expression in Triple-Negative Breast Cancer. *Diagnostics (Basel)* 2022;*12*(2).
36. Okada, Y.; Suzuki, H.; Tanaka, T.; Kaneko, M.K.; Kato, Y. Epitope Mapping of an Anti-Mouse CD39 Monoclonal Antibody Using PA Scanning and RIEDL Scanning. *Monoclon Antib Immunodiagn Immunother* 2024;*43*(2): 44-52.
37. Asano, T.; Kaneko, M.K.; Takei, J.; Tateyama, N.; Kato, Y. Epitope Mapping of the Anti-CD44 Monoclonal Antibody (C(44)Mab-46) Using the REMAP Method. *Monoclon Antib Immunodiagn Immunother* 2021;*40*(4): 156-161.
38. Asano, T.; Kaneko, M.K.; Kato, Y. Development of a Novel Epitope Mapping System: RIEDL Insertion for Epitope Mapping Method. *Monoclon Antib Immunodiagn Immunother* 2021;*40*(4): 162-167.
39. Sano, M.; Kaneko, M.K.; Aasano, T.; Kato, Y. Epitope Mapping of an Antihuman EGFR Monoclonal Antibody (EMab-134) Using the REMAP Method. *Monoclon Antib Immunodiagn Immunother* 2021;*40*(4): 191-195.
40. Nanamiya, R.; Sano, M.; Asano, T.; et al. Epitope Mapping of an Anti-Human Epidermal Growth Factor Receptor Monoclonal Antibody (EMab-51) Using the RIEDL Insertion for Epitope Mapping Method. *Monoclon Antib Immunodiagn Immunother* 2021;*40*(4): 149-155.
41. Zhou, Y.; Yamada, N.; Tanaka, T.; et al. Crucial roles of RSK in cell motility by catalysing serine phosphorylation of EphA2. *Nat Commun* 2015;*6*: 7679.
42. Miao, H.; Li, D.Q.; Mukherjee, A.; et al. EphA2 mediates ligand-dependent inhibition and ligand-independent promotion of cell migration and invasion via a reciprocal regulatory loop with Akt. *Cancer Cell* 2009;*16*(1): 9-20.
43. Macrae, M.; Neve, R.M.; Rodriguez-Viciana, P.; et al. A conditional feedback loop regulates Ras activity through EphA2. *Cancer Cell* 2005;*8*(2): 111-118.
44. Harly, C.; Joyce, S.P.; Domblides, C.; et al. Human γδ T cell sensing of AMPK-dependent metabolic tumor reprogramming through TCR recognition of EphA2. *Sci Immunol* 2021;*6*(61).
45. Koshikawa, N.; Hoshino, D.; Taniguchi, H.; et al. Proteolysis of EphA2 Converts It from a Tumor Suppressor to an Oncoprotein. *Cancer Res* 2015;*75*(16): 3327-3339.
46. Chen, Z.; Liu, Z.; Zhang, M.; et al. EPHA2 blockade reverses acquired resistance to afatinib induced by EPHA2-mediated MAPK pathway activation in gastric cancer cells and avatar mice. *Int J Cancer* 2019;*145*(9): 2440-2449.
47. Mitra, D.; Bhattacharyya, S.; Alam, N.; et al. Phosphorylation of EphA2 receptor and vasculogenic mimicry is an indicator of poor prognosis in invasive carcinoma of the breast. *Breast Cancer Res Treat* 2020;*179*(2): 359-370.
48. Ishikawa, K.; Suzuki, H.; Ohishi, T.; et al. Antitumor activities of anti-CD44 monoclonal antibodies in mouse xenograft models of esophageal cancer. *Oncol Rep* 2024;*52*(5).
49. Ishikawa, K.; Suzuki, H.; Ohishi, T.; et al. Anti-CD44 Variant 10 Monoclonal Antibody Exerts Antitumor Activity in Mouse Xenograft Models of Oral Squamous Cell Carcinomas. *Int J Mol Sci* 2024;*25*(17).
50. Cioce, M.; Fazio, V.M. EphA2 and EGFR: Friends in Life, Partners in Crime. Can EphA2 Be a Predictive Biomarker of Response to Anti-EGFR Agents? *Cancers (Basel)* 2021;*13*(4).
51. Jin, P.; Zhang, J.; Sumariwalla, P.F.; et al. Novel splice variants derived from the receptor tyrosine kinase superfamily are potential therapeutics for rheumatoid arthritis. *Arthritis Res Ther* 2008;*10*(4): R73.
52. Lévêque, R.; Corbet, C.; Aubert, L.; et al. ProNGF increases breast tumor aggressiveness through functional association of TrkA with EphA2. *Cancer Lett* 2019;*449*: 196-206.
53. Li, Y.; Peng, Q.; Wang, L. EphA2 as a phase separation protein associated with ferroptosis and immune cell infiltration in colorectal cancer. *Aging (Albany NY)* 2023;*15*(22): 12952-12965.

 doi:10.20944/preprints202410.0572.v1

54. Boissier, P.; Chen, J.; Huynh-Do, U. EphA2 signaling following endocytosis: role of Tiam1. *Traffic* 2013;*14*(12): 1255-1271.
55. Marco, S.; Neilson, M.; Moore, M.; et al. Nuclear-capture of endosomes depletes nuclear G-actin to promote SRF/MRTF activation and cancer cell invasion. *Nat Commun* 2021;*12*(1): 6829.